1   The chimeric TAC receptor co-opts the T cell receptor yielding robust anti-tumor activity
2   without toxicity
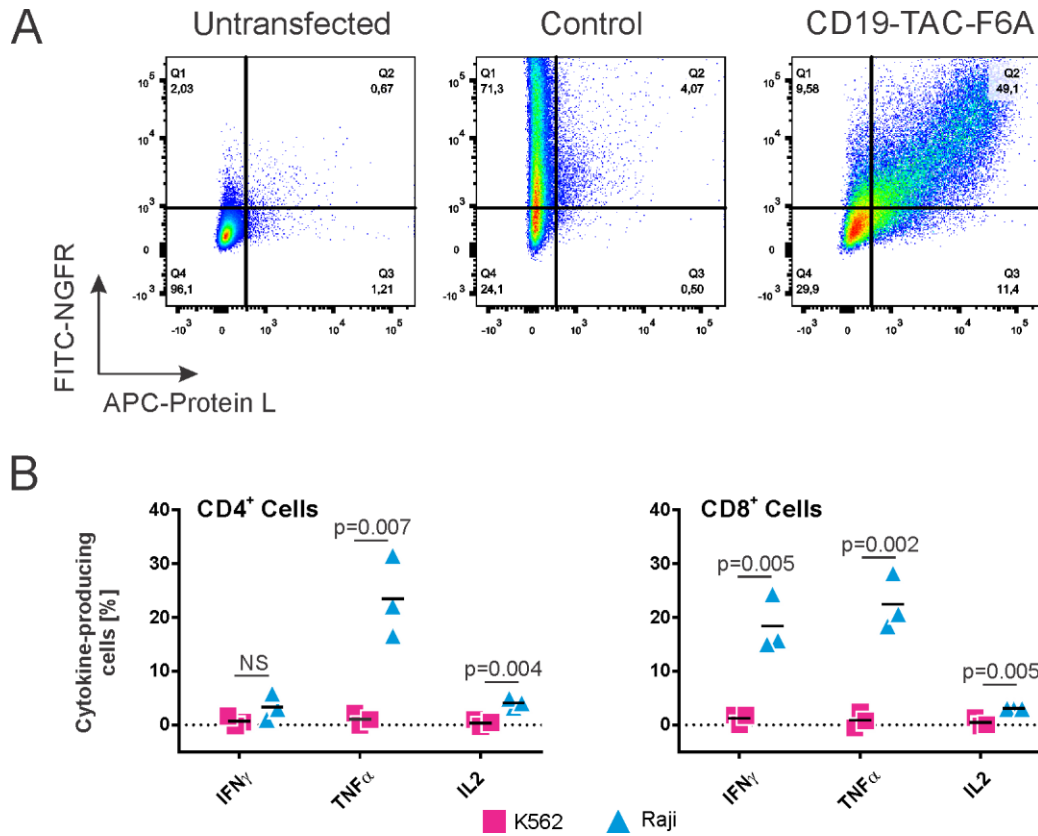
3

4

5   **Helsen et al.**
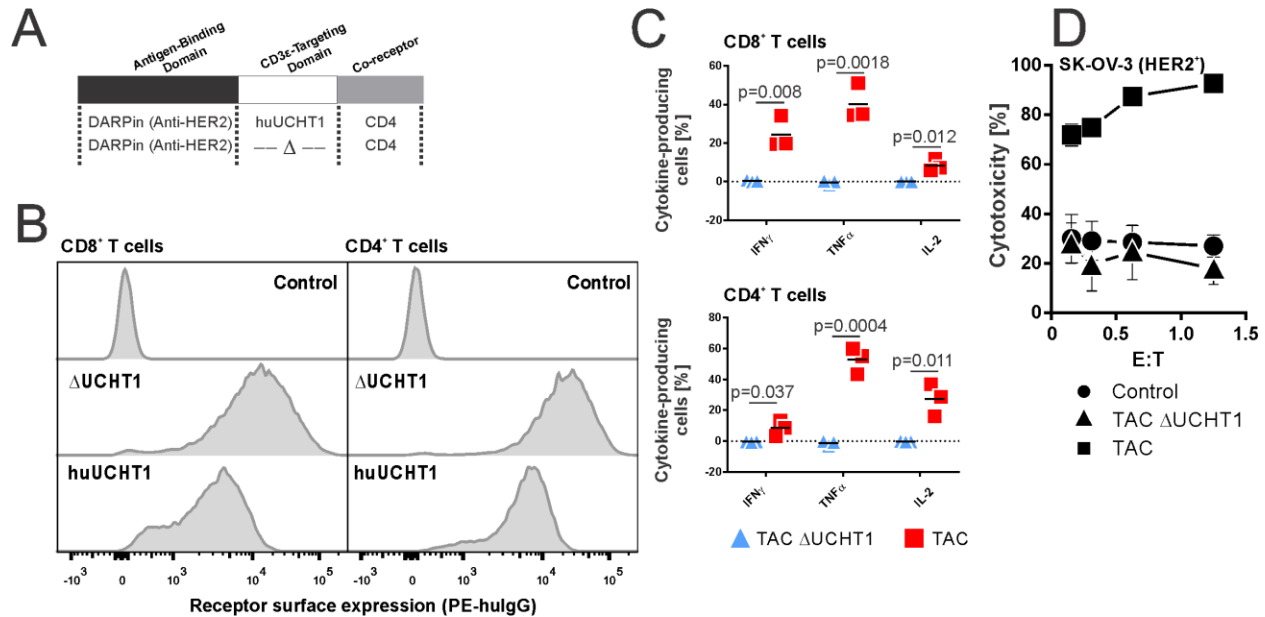
Supplementary Figures

Supplementary Figure 1:

F6A scFv TAC can be detected by Protein L and F6A TAC engineered T cells show antigen specific reactivity. **A.** Protein L binds the kappa light chain of scFv. HEK 293T cells were transfected with CD19-TAC-F6A, stained and analyzed for TAC and tNGFR expression by flow cytometry. For the gating strategy see Supplementary Fig. 16. **B.** CD19-TAC-cells were stimulated with antigen-positive Raji (triangle) or antigen-negative K562 (square) tumor cells, respectively. Data are presented as percent of CD4 or CD8 T cells producing cytokine. Lines represent data medians. Multiple t-test was used to determine significance. For the gating strategy see Supplementary Fig. 13B.

20

21

22

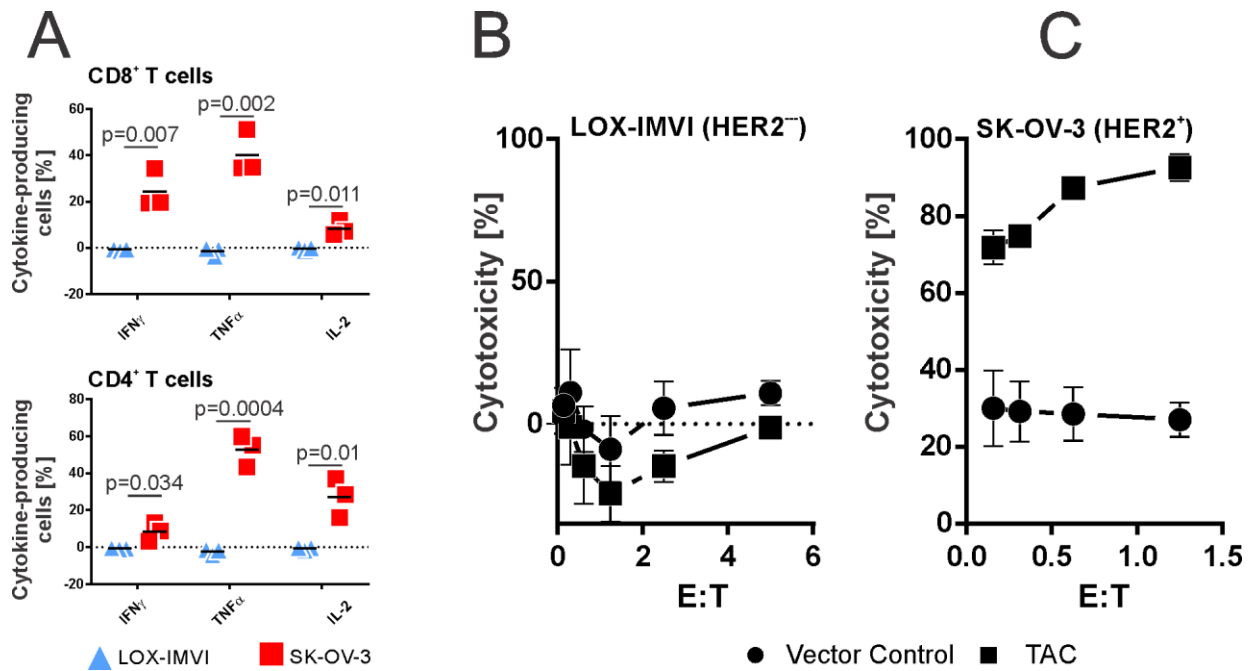Supplementary Figure 2:

CD3-binding domain is required for TAC-engineered T cell function. Full-length and ΔUCHT1 TAC receptors (**A**) were expressed on the surface of primary human T cells (**B**). Relative TAC surface expression is measured by flow cytometry. Cells were stained for CD4, CD8, tNGFR and TAC (via its Myc Tag), and gated on either CD4+NGFR+ or CD8+NGFR+; representative TAC expression data are presented as histograms. For the gating strategy see Supplementary Fig. 13A. **C**. HER2-TAC-T cells (bearing huUCHT1 (square) or ΔUCHT1 (triangle)) are stimulated with antigen-positive SK-OV-3 tumor cells. Data are presented as percent of CD4+ or CD8+ T cells producing cytokine. Lines represent data means. Multiple t-test was used to determine significance. For the gating strategy see Supplementary Fig. 13B. **D**. HER2-TAC-T cells (bearing huUCHT1 (square) or ΔUCHT1 (triangle)) and vector control T cells (circles) are co-cultured with SK-OV-3 tumor cells to measure TAC-T cell-mediated cytotoxicity. Data are from 3 independent experiments with 3 different donors; error bars show standard deviation.

38

41

42 Supplementary Figure 3:

43 **TAC-T cells show no evidence of auto-activation in the absence of target antigen.** Data

44 originates from the same experiment as Supplemental Figure 2. **A**. HER2-TAC-T cells are

45 stimulated with antigen-positive SK-OV-3 (square) or antigen-negative LOX-IMVI (triangle)

46 tumor cells. Data are presented as percent of CD4$^+$ or CD8$^+$ T cells producing cytokine. Lines

47 represent data means. Multiple t-test was used to determine significance. For the gating strategy

48 see Supplementary Fig. 13B. **B-C**. HER2-TAC-T cells (bearing UCHT1; square) and vector

49 control T cells (circle) are co-cultured with LOX-IMVI or SK-OV-3 tumor cells to measure

50 TAC-T cell-mediated cytotoxicity. Data are from 3 independent experiments with 3 different

51 donors; error bars show standard deviation.

52

53

54

55
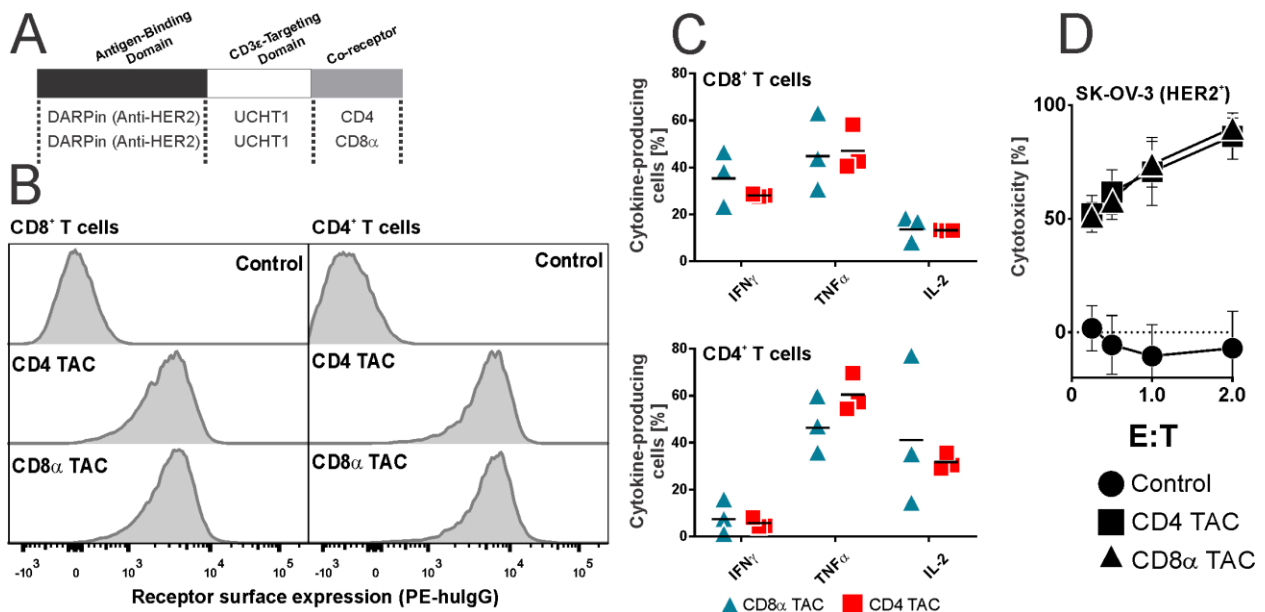
Supplementary Figure 4:

Evaluation of cytosolic TAC domains. **A**. Schematic representation of CD4 and CD8α TAC constructs containing the anti-HER2 DARPin and UCHT1 CD3-binding domain. **B**. Cells were stained for CD4, CD8, tNGFR, and TAC expression, and gated on either CD4+NGFR+ or CD8+NGFR+; representative TAC expression data are presented as histograms. For the gating strategy see Supplementary Fig. 13A. **C**. Cytokine production by CD4 TAC- (square) and CD8α TAC- (triangle) T cells stimulated by HER2+ SK-OV-3 tumor cells are shown. Lines represent data means. Multiple t-test was used to determine significance. For the gating strategy see Supplementary Fig. 13B. **D.** Cytotoxicity was measured by co-culturing HER2+ SK-OV-3 tumor cells with TAC- (CD4 co-receptor (squares) or CD8α co-receptor (triangles)) or vector control (circles) T cells. Data are from 3 independent experiments with 3 different donors; error bars show standard deviation.
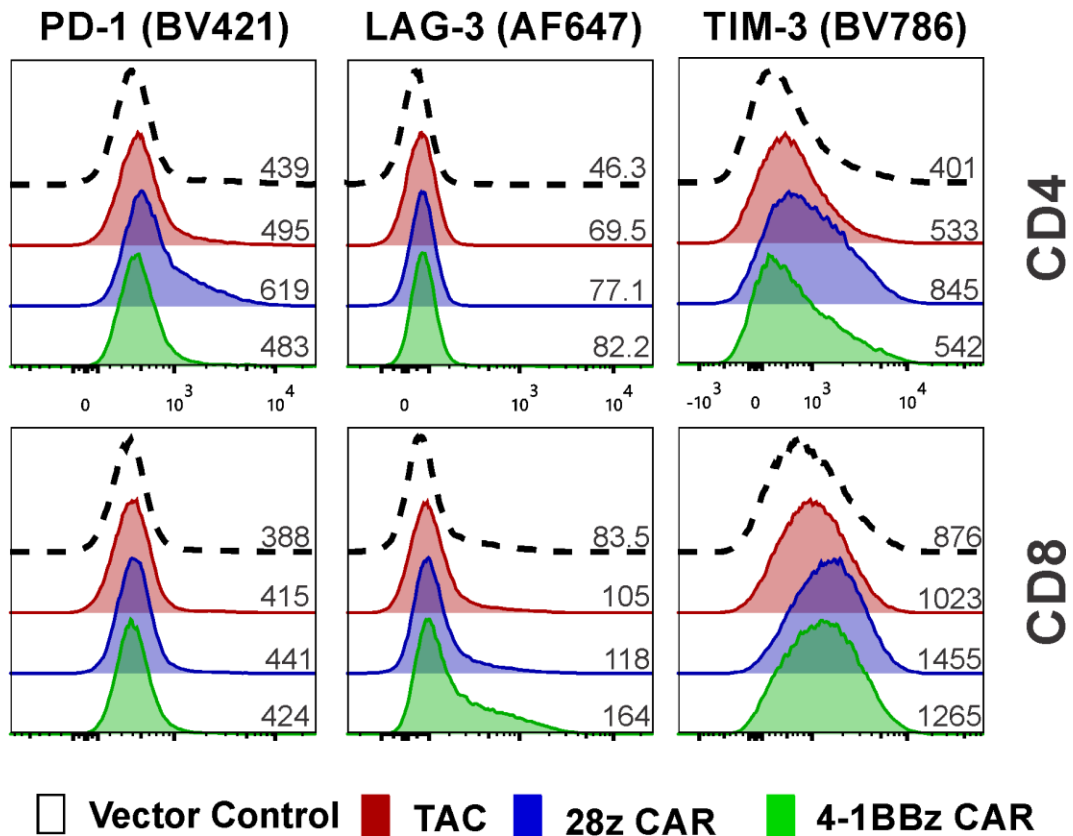
68

69
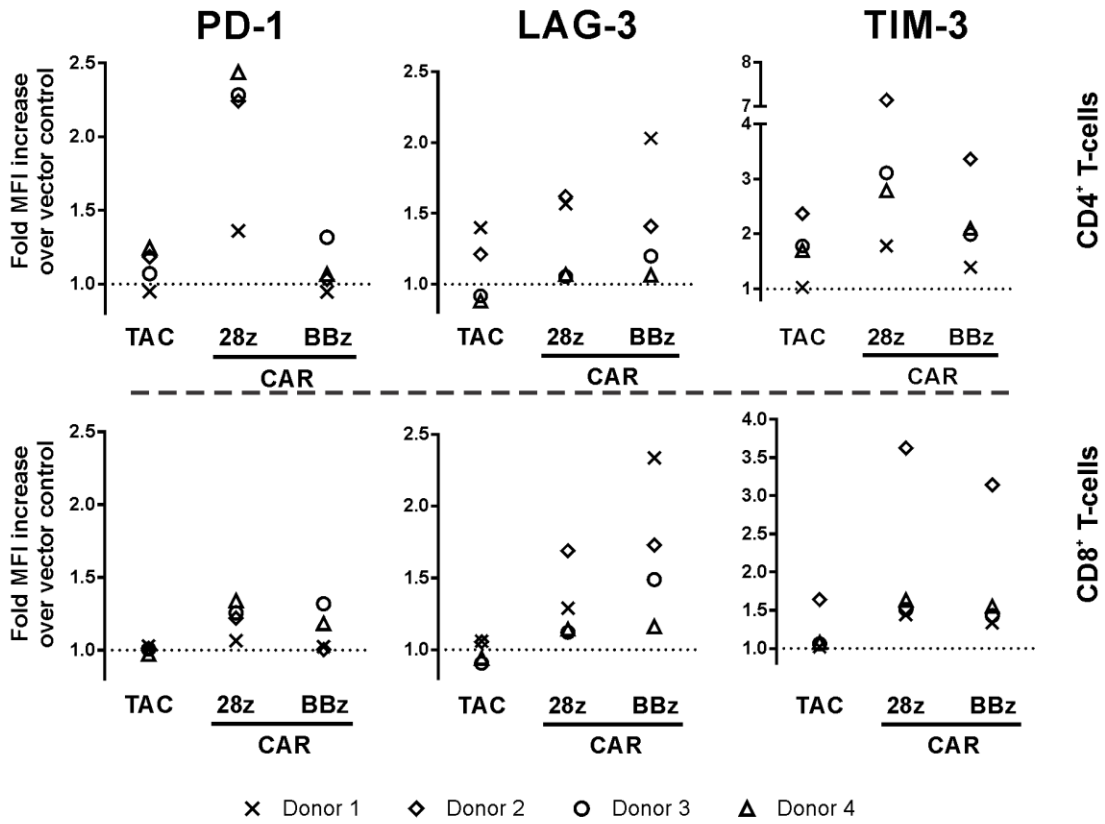
71 Supplementary Figure 5:

72 **Relative expression of checkpoint receptors in CAR- and TAC-engineered T cells**. T cells

73 are transduced with HER2-TAC, anti-HER2 28ζ CAR or anti-HER2 BBζ CAR, stained for

74 surface marker expression, and analyzed by flow cytometry. **A.** Expression of checkpoint

75 receptors PD-1, LAG-3 and TIM-3. Populations are gated on either $CD4^+NGFR^+$ or

76 $CD8^+NGFR^+$. All data are normalized to vector control (vector only carrying tNGFR). Data is

77 derived from 4 individual donors across two separate experiments. Each donor is represented by

78 a unique symbol to visualize donor-to-donor variations. **B.** Representative histograms of HER2-

79 TAC (red), anti-HER2 28ζ CAR (blue) or anti-HER2 BBζ CAR (green). Populations are gated on

80 either $CD4^+NGFR^+$ or $CD8^+NGFR^+$. Representative, normalized histograms per marker are

81 shown. Values shown indicate mean fluorescence intensity. For both A and B the gating strategy

82 is shown in Supplementary Fig. 14.

83

A

Antigen-Binding Domain	CD3ε-Targeting Domain	Co-receptor
DARPin (Anti-HER2)	UCHT1	CD4

TAC

Antigen-Binding Domain	Hinge/TM	Cytoplasmic
DARPin (Anti-Her2)	CD8	CD3ζ

1st Gen CAR :

B

CD8+ T cells

Cytokine-producing cells [%]

IFNγ   TNFα

CD4+ T-cells

Cytokine-producing cells [%]

IFNγ   TNFα

■ TAC   ▲ 1st Gen CAR

C

LOX-IMVI (HER2⁻)   OVCAR-3 (HER2⁺)

Cytotoxicity [%]   Cytotoxicity [%]

E:T   E:T

● Vector Control   ▲ 1st Gen CAR   ■ TAC

D

Antigen-Binding Domain	CD3ε-Targeting Domain	Co-receptor
DARPin (Anti-HER2)	UCHT1	CD4

TAC

Antigen-Binding Domain	Hinge/TM	Cytoplasmic
DARPin (Anti-HER2)	CD8/CD28	CD28/CD3ζ

2st Gen CAR :

E

CD8+ T cells

Cytokine-producing cells [%]

IFNγ   TNFα   IL-2

CD4+ T cells

Cytokine-producing cells [%]

IFNγ   TNFα   IL-2

▼ 2nd Gen CAR   ■ TAC

F

LOX-IMVI (HER2⁻)   OVCAR-3iv (HER2⁺)

Cytotoxicity [%]   Cytotoxicity [%]

E:T   E:T

● Vector Control   ■ TAC   ▼ 2nd Gen CAR

84

85   Supplementary Figure 6:

86   **First-generation CAR-, second-generation CAR-, and TAC-T cells exhibit similar *in vitro***

87   **potency. A.** Schematics of TAC and first-generation CAR constructs. **B.** Comparison of cytokine

88   production from $CD4^+$ or $CD8^+$ TAC- (square) and first-generation CAR- (triangle) T cells when

89   stimulated with $HER2^+$ OVCAR-3 tumor cells (minus cytokine production triggered by $HER2^-$

90   LOX-IMVI tumor cells). Lines represent data means. **C.** Cytotoxicity of TAC- (square) and first-

91   generation CAR- (triangle) relative to vector control (circle) T cells against OVCAR-3 and

92   LOX-IMVI tumor cells. Data are from 3-4 independent experiments; error bars show standard

93   error of the mean. **D.** Schematics of the TAC and second-generation CD28-based CAR

94   constructs. **E.** Comparison of cytokine production from $CD4^+$ or $CD8^+$ TAC- (square) and

95   second-generation CAR- (inverted triangle) T cells when stimulated with OVCAR-3 (minus

96   cytokine production triggered by $HER2^-$ LOX-IMVI tumor cells). Lines represent data means. **F.**
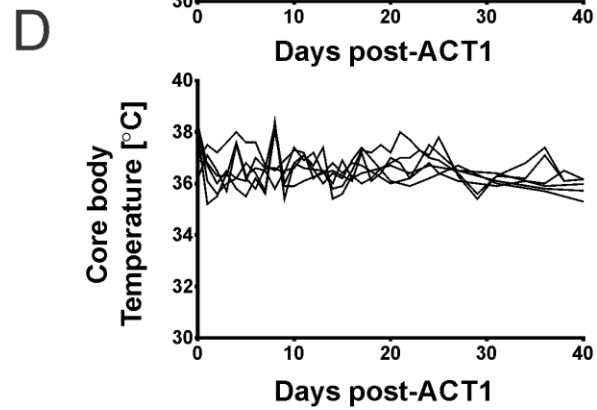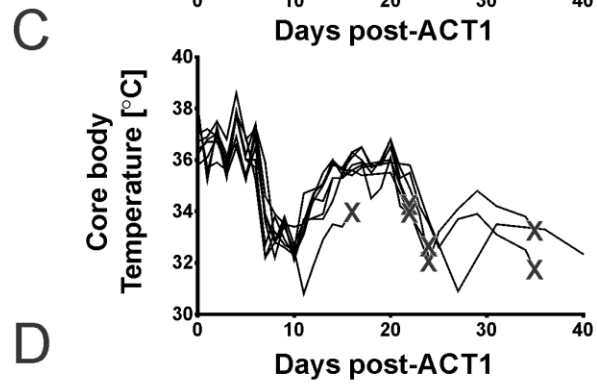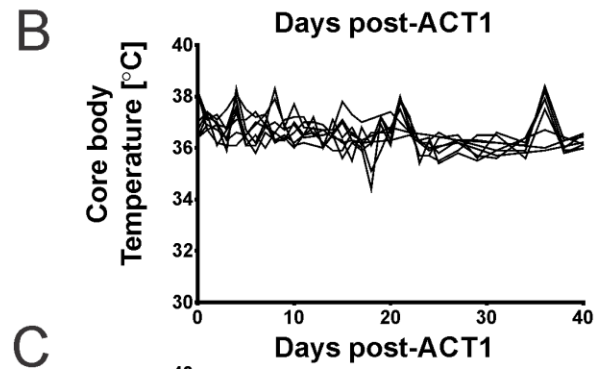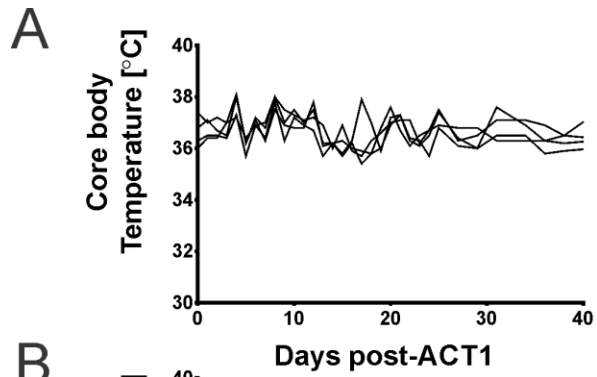
97   Cytotoxicity of TAC- (square) and second-generation CD28-based CAR- (inverted triangle)

98   relative to vector control (circle) T cells against LOX-IMVI and OVCAR-3 tumor cells. Data are
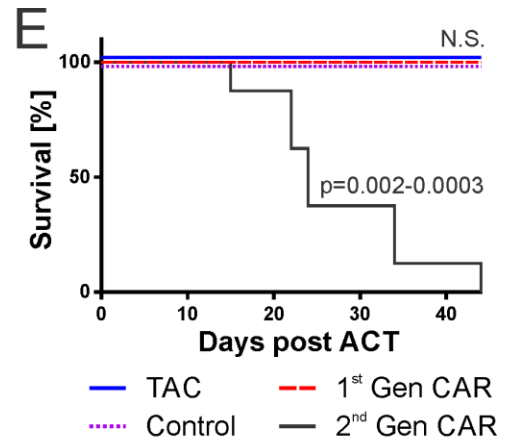
99   from 3 independent experiments; error bars show standard error of the mean. For B and E the

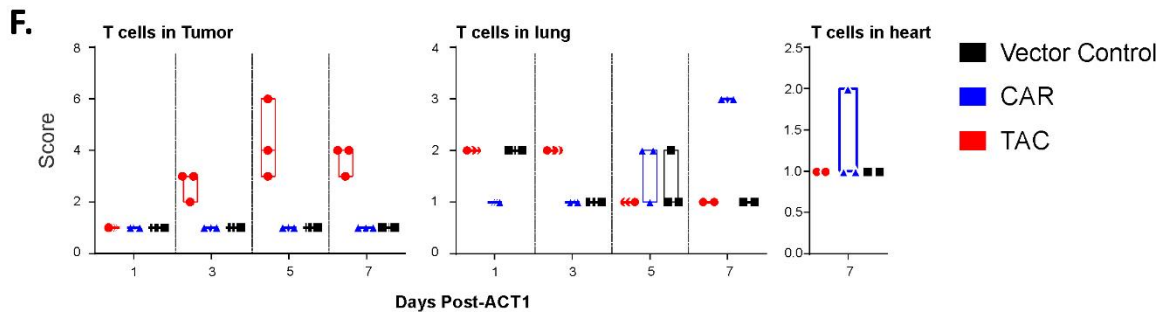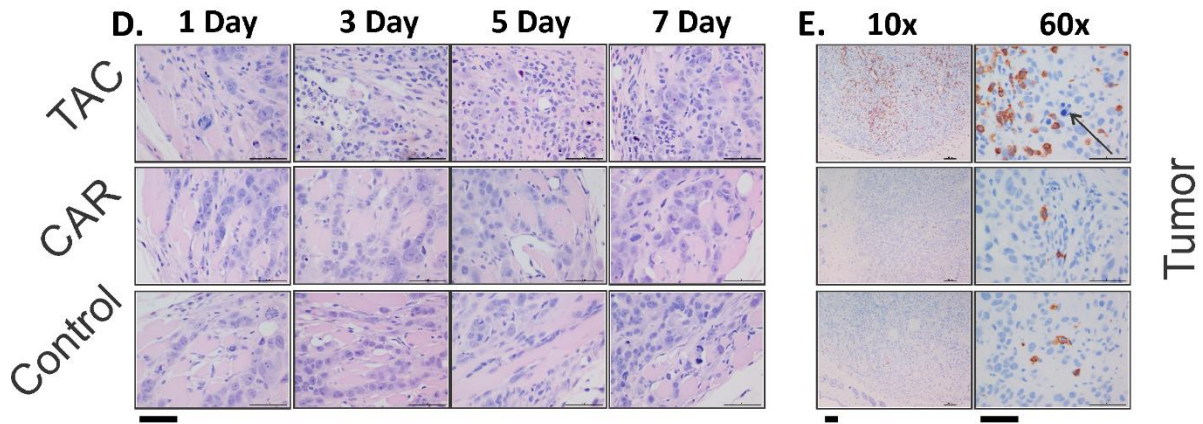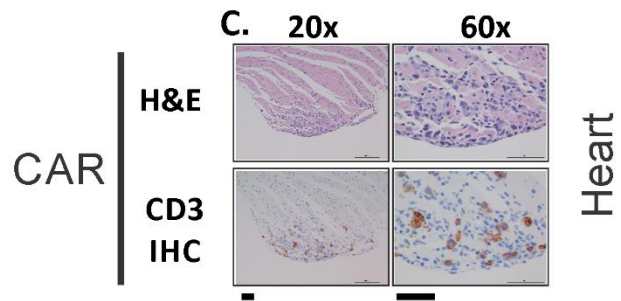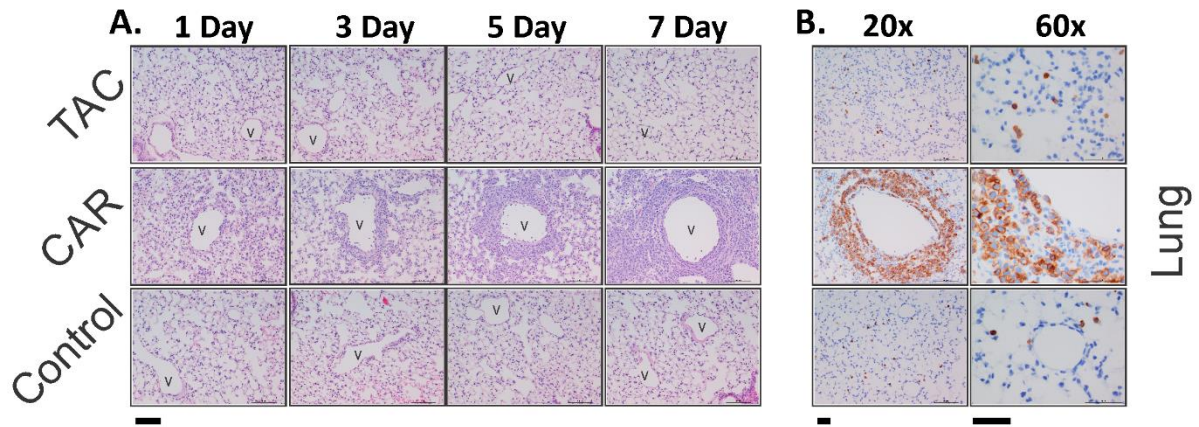100 gating strategy is shown if Supplementary Fig. 13B.

101

102

103

104

105

106

107

108   Supplementary Figure 7:

109   **HER2-TAC-T cells demonstrate an enhanced safety profile over first- and second-**

110   **generation HER2-CAR-T cells** *in vivo*. OVCAR-3 tumor-bearing mice are treated with 2.0×10^6

111   HER2-TAC-T cells (**A**), first-generation anti-HER2 CAR-T cells (**B**), second-generation anti-

112   HER2 28ζ CAR-T cells (**C**), or a matched total number of vector control T cells (**D**). Mice are

113   followed for change in core body temperature; each curve displays data from a single treated

114   mouse. When mice reach a toxicity-induced endpoint, this is indicated via an X. Data has been

115   replicated in an additional independent experiment. The change in core body temperature

116   between vector control, 1st gen CAR, and TAC was not significantly different. Significance was

117   determined via curve fitting and multiple t-test. Survival is shown in (**E**). Vector control (purple,

118   dotted), TAC (blue, solid) or first-generation CAR (red, dashes) treated mice showed no toxicity-

119   induced endpoints and were not significantly different. In contrast, second-generation 28ζ CAR

120   (black, solid)-treated mice all reached toxicity-induced endpoint within 44 days. Mice were not

121   followed to tumor volume endpoint. Significance was determined via the Log Rank test.

122

123

A. 1 Day 3 Day 5 Day 7 Day
TAC / CAR / Control — Lung

B. 20x 60x — Lung

C. CAR 20x 60x H&E CD3 IHC — Heart

D. 1 Day 3 Day 5 Day 7 Day
TAC / CAR / Control — Tumor

E. 10x 60x — Tumor

F. T cells in Tumor, T cells in lung, T cells in heart
Score vs Days Post-ACT1
Vector Control, CAR, TAC

127 Supplementary Figure 8:

128 **TAC- and CAR-T cells show differential patterns of localization *in vivo*.** OVCAR-3 tumor-

129 bearing mice were treated with $6.0{\times}10^6$ second-generation anti-HER2 28ζ CAR- or HER2-TAC-

130 T cells, or a matched total number of vector control T cells. At 1, 3, 5, and 7 days post-ACT1

131 mice (n = 3 per treatment) were perfused and tissues were formalin fixed and paraffin embedded.

132 **A.** Timecourse of H&E (hematoxylin and eosin) stained lung sections at 20X magnification;

133 vasculature is indicated by a "v". Scale bar indicates $100\,\mu$m. **B.** CD3 IHC staining of lung

134 sections at 7 days post-ACT1. Scale bar indicates $50\,\mu$m**. C.** H&E and CD3 IHC of cardiac tissue

135 at 7 days post-ACT1. Scale bar indicates $50\,\mu$m. **D.** Timecourse of H&E stained tumor sections

136 at 60X magnification. Scale bar indicates $50\,\mu$m. **E.** CD3 IHC staining of tumor sections at 7

137 days post-ACT1; arrow indicates a necrotic tumor cell. Scale bar indicates $50\,\mu$m. In all cases,

138 images are representative of observations in all mice (n = 3 each). **F.** CD3 IHC was performed

139 on heart, lung, and tumor tissue; T cell infiltrate was scored as % infiltrate based on tissue area in

140 10% intervals (score 1 = <1%, score 2 = 1-10%, score 3 = 10-20%, score 4 = 20-30%, score 5 =

141 30-40%, and score 6 = 40-50%). Data presented as an average score for n = 3 mice per time
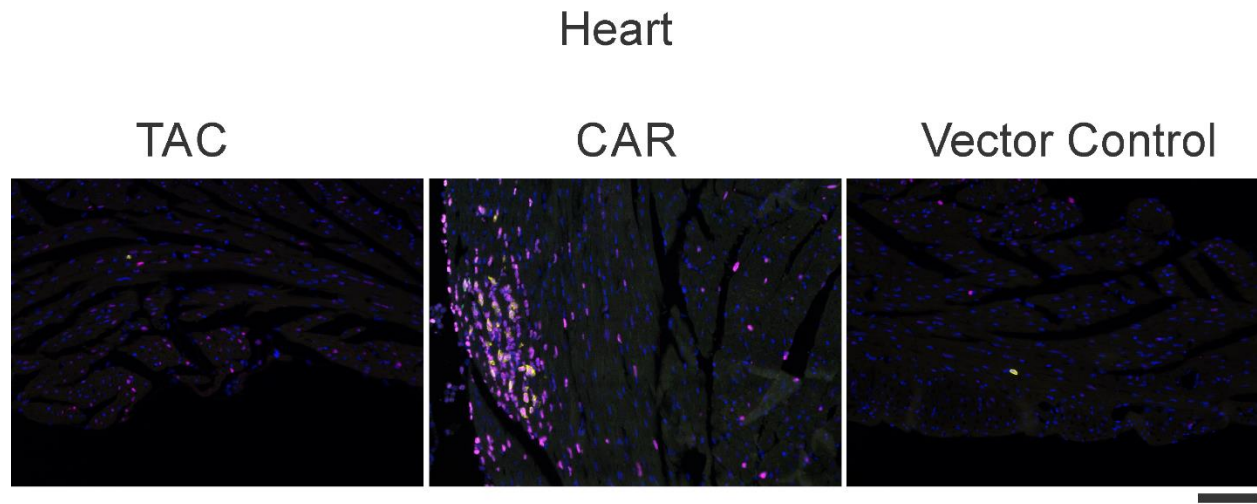
142 point.

143
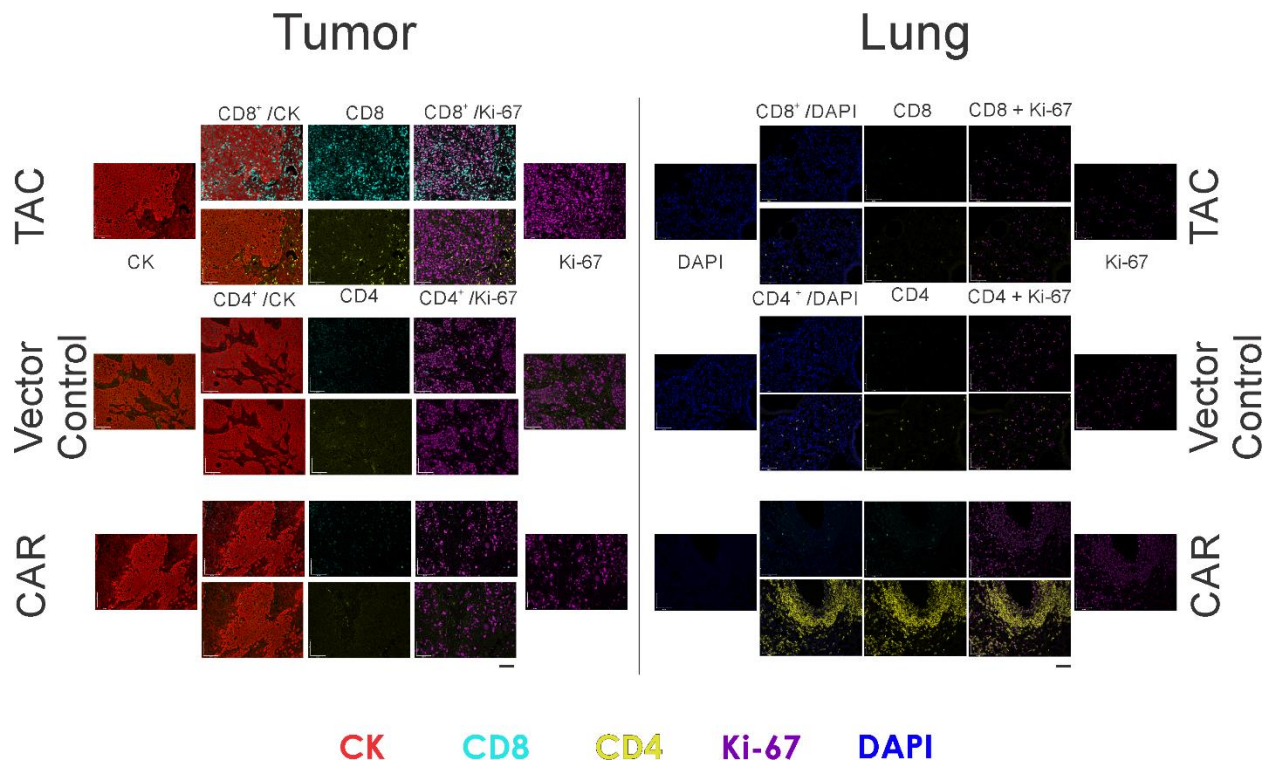
Supplementary Figure 9:

Single color and composite multicolor IHC tissue analysis. OVCAR-3 tumor-bearing mice were treated with 6.0×10^6 second-generation anti-HER2 28ζ CAR- or HER2-TAC-T cells, or a matched total number of vector control T cells. At 7 days post-ACT1 mice (n = 3 per treatment) were perfused and tissues were formalin fixed and paraffin embedded for subsequent multicolor IHC analysis (tumor or lung tissues were stained for human cytokeratin (CK, red), cellular proliferation marker Ki-67 (purple), CD8 (cyan), CD4 (yellow), and DAPI (blue)). Representative single-color images are shown alongside 2-color overlay images. Scale bar indicates 100 μm.

156

Heart

| TAC | CAR | Vector Control |

CD8 **CD4** **Ki-67** **DAPI**

157

158 Supplementary Figure 10:

159 **Multicolor IHC of cardiac tissue at 7 days post-ACT1**. OVCAR-3 tumor bearing mice were

160 treated with 6.0×10^6 second-generation anti-HER2 28ζ CAR- or HER2-TAC-T cells, or a

161 matched total number of vector control T cells. At 7 days post-ACT1 mice (n = 3 per treatment)

162 were perfused and tissues were formalin fixed and paraffin embedded for subsequent multicolor

163 IHC analysis (cardiac tissue was stained for cellular proliferation marker Ki-67 (purple), CD8

164 (cyan), CD4 (yellow), and DAPI (blue)). Scale bar indicates 100 μm. Representative images are
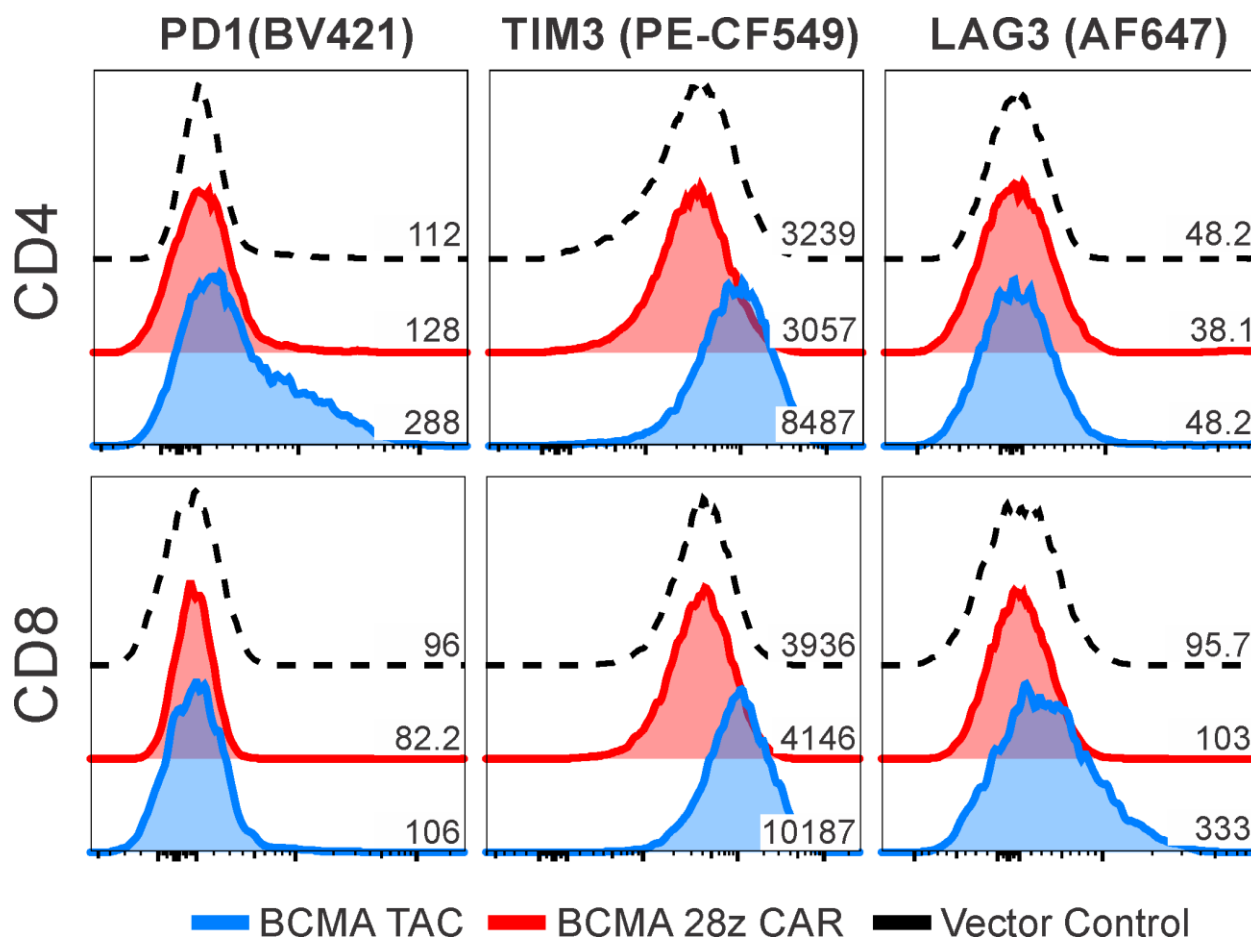
165 shown.

166
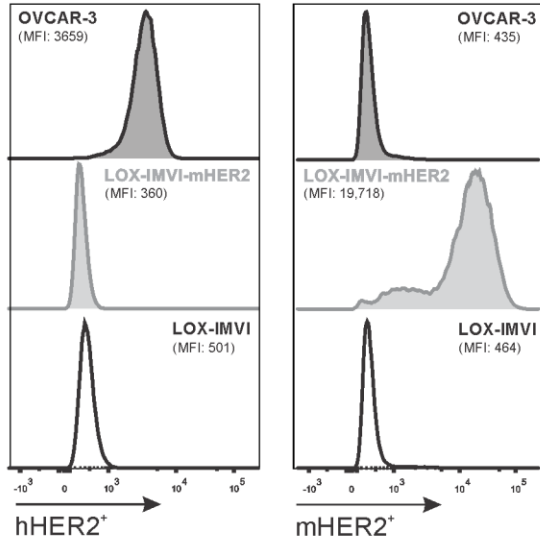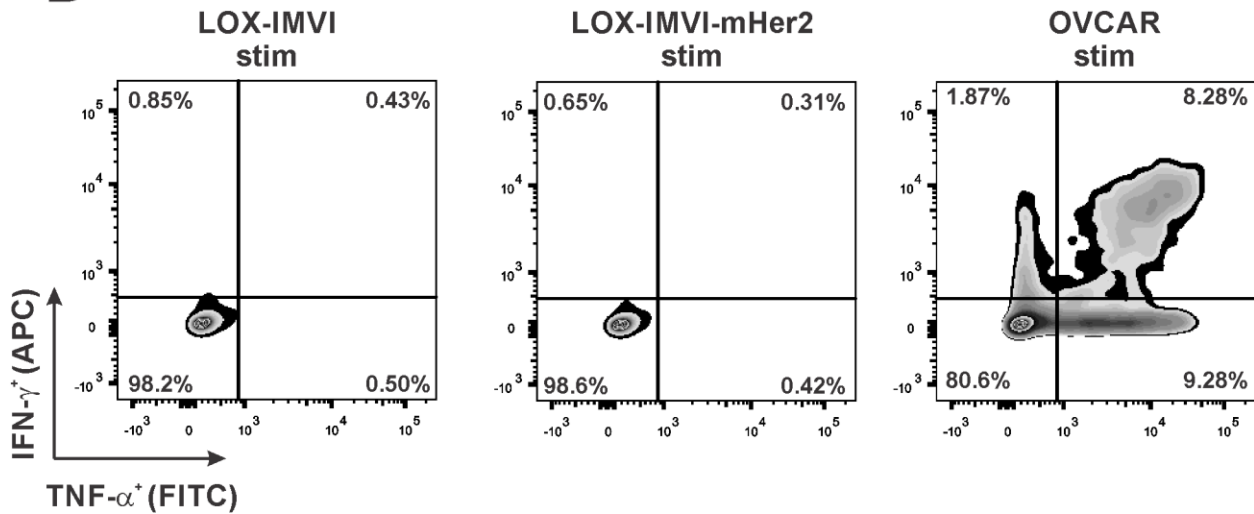
167
168
169
170 Supplementary Figure 11.
171 **Second generation anti-HER2 28ζ CAR-T cells do not respond to murine HER2. A.**
172 Expression of human or murine HER2 (hHER2 or mHER2, respectively) on OVCAR-3, LOX-
173 IMVI, and LOX-IMVI-mHER2 tumor cell lines as determined by flow cytometry. For the gating
174 strategy see Supplementary Fig. 16. **B.** Production of activation cytokines (IFN-γ and TNF-α) by
175 CD8^{+} CD28ζ-CAR T cells after stimulation with tumor cell lines (as indicated) was determined
176 by flow cytometry. Data is representative of findings from two independent experiments. For the
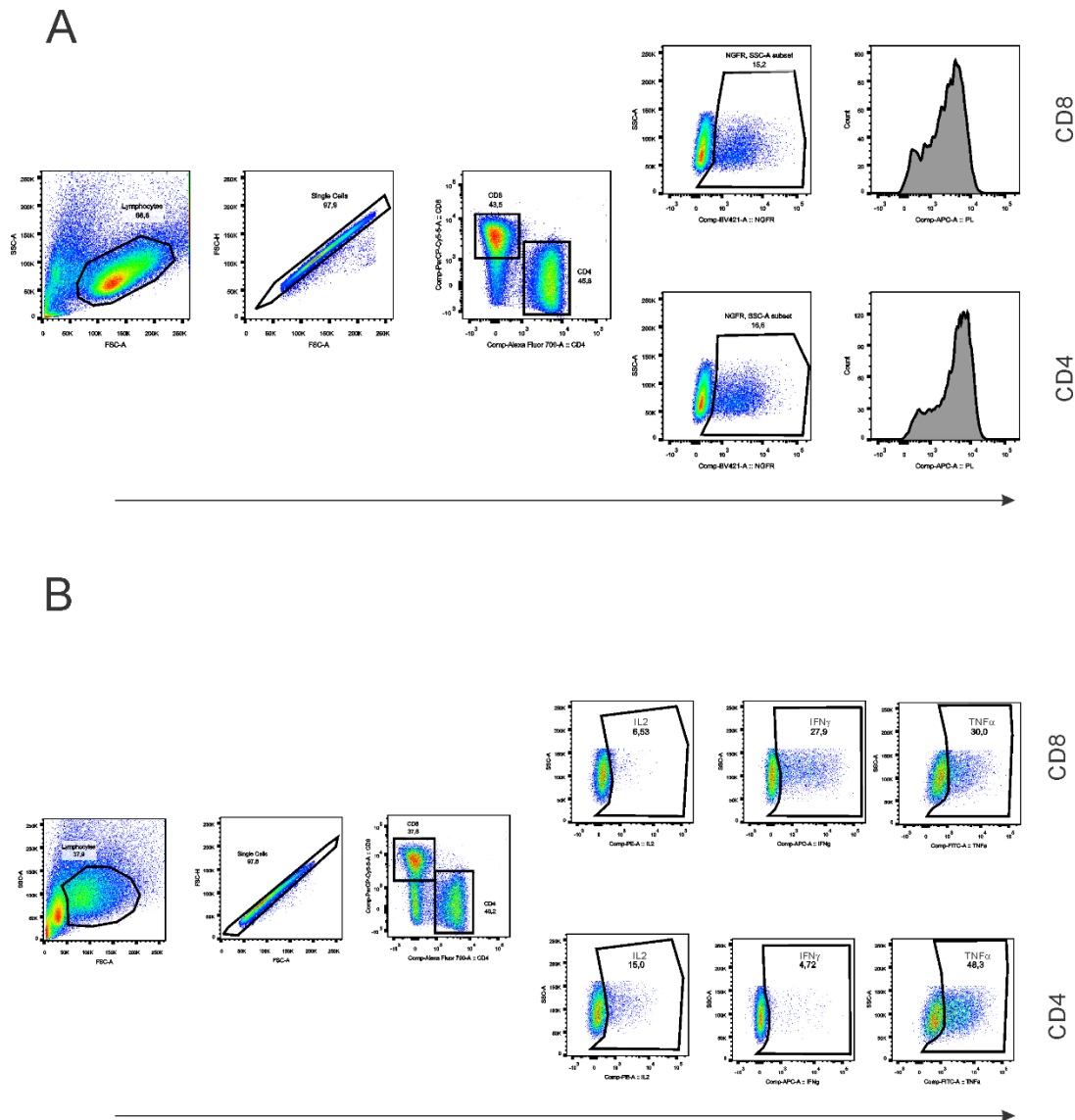177 gating strategy see Supplementary Fig. 13B.
178

PD1(BV421) | **TIM3 (PE-CF549)** | **LAG3 (AF647)**

CD4 — PD1: 112, 128, 288; TIM3: 3239, 3057, 8487; LAG3: 48.2, 38.1, 48.2

CD8 — PD1: 96, 82.2, 106; TIM3: 3936, 4146, 10187; LAG3: 95.7, 103, 333

BCMA TAC — BCMA 28z CAR — Vector Control

Supplementary Figure 12:

Relative expression of checkpoint receptors in BCMA-CAR- and TAC-engineered T cells.
T cells were transduced with BCMA-TAC, second-generation BCMA-CD28ζ-CAR, or vector
control (tNGFR). Engineered T cells are stained for surface marker expression and analyzed by
flow cytometry. Populations are gated on CD4$^+$NGFR$^+$ or CD8$^+$NGFR$^+$ analysis. Values indicate
MFI of each marker. Histograms are from one donor, representative of three donors from three
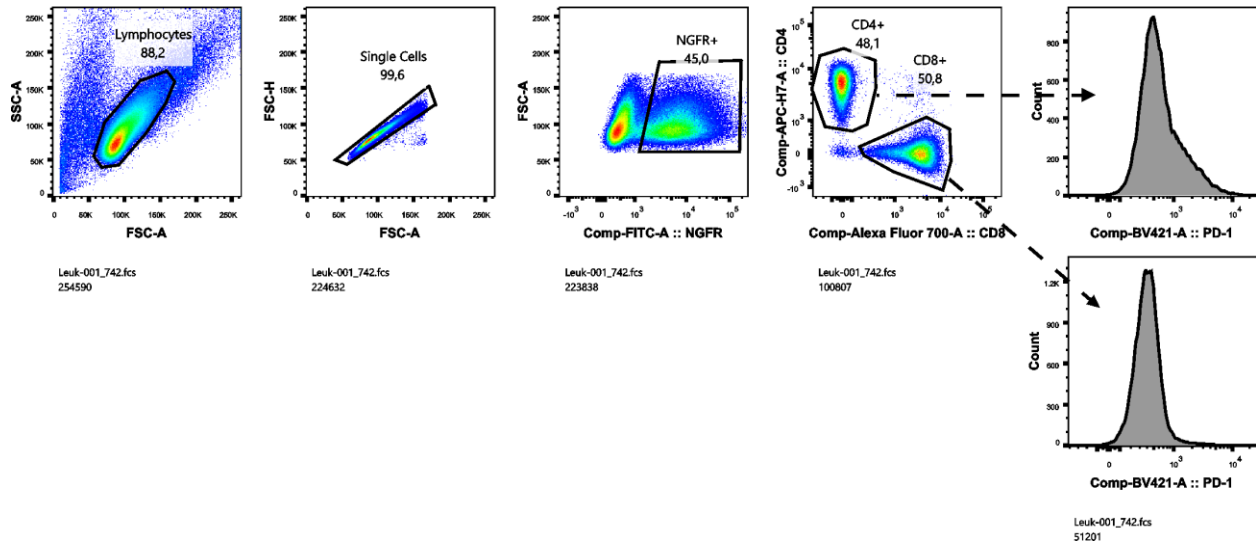independent experiments. For the gating strategy see Supplementary Fig. 14

194

195

196 Supplementary Figure 13:

197 **Examples of gating strategies used for the analysis of flow cytometry data. A.** Gating

198 strategy for phenotypic analysis of engineered T cells. Lymphocytes (SSC-A v. FSC-A) →

199 singlets (FSC-H v. FSC-A) → CD8^{+} *or* CD4^{+} cells (CD8-PerCPCy5.5 v. CD4-AF700) →

200 NGFR^{+} cells (SSC-A v. NGFR-BV421) → TAC receptor expression as a histogram (Protein L^{+}

201 with indirect detection via APC-conjugated streptavidin is shown as an example). NGFR[+] gates

202 were set based on fully stained, non-transduced T cell controls. **B.** Gating strategy for functional

203 cytokine production by tumor cell line-stimulated engineered T cells. Lymphocytes (SSC-A v.

204 FSC-A) → singlets (FSC-H v. FSC-A) → CD8^{+} *or* CD4^{+} cells (CD8-PerCPCy5.5 v. CD4-

205 AF700) → cytokine positive (SSC-A v. TNF-α-FITC *or* IFN-γ-APC *or* IL-2-PE). Cytokine^{+}

206 gates were set based on fully stained, PBS- or antigen-negative tumor cell line-stimulated
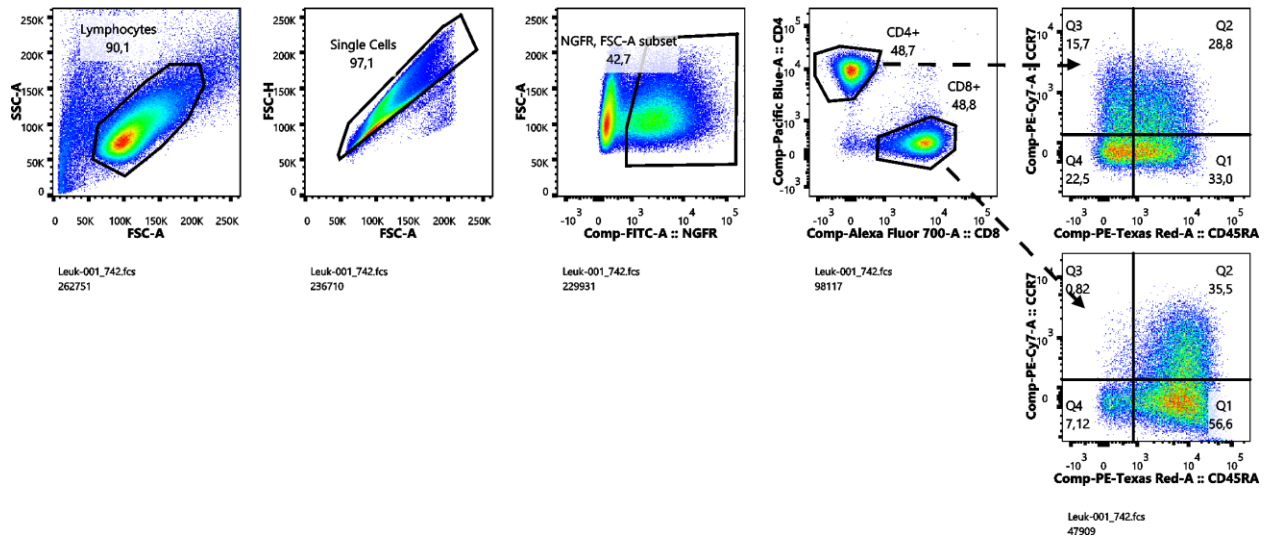
207 controls.

208

209

210   Supplementary Figure 14:

211   **Examples of gating strategies used for the analysis of flow cytometry data.** Gating strategy
212   for checkpoint analysis of engineered T cells. Lymphocytes (SSC-A v. FSC-A) → singlets (FSC-
213   H v. FSC-A) → NGFR$^+$ cells (SSC-A v. NGFR- VioBright FITC) → CD8$^+$ *or* CD4$^+$ cells (CD8-
214   AF700 v. CD4-APC-H7-A) → Checkpoint receptor expression as a histogram (TIM-3-BV785/
215   LAG-3-AF647/ PD-1-BV421). NGFR+ gates were set based on fully stained, vector control
216   transduced T cells.

217

218

219

220

221

222 Supplementary Figure 15:

223 **Examples of gating strategies used for the analysis of flow cytometry data.** Gating strategy
224 for memory population analysis of engineered T cells. Lymphocytes (SSC-A v. FSC-A) →
225 singlets (FSC-H v. FSC-A) → NGFR$^+$ cells (SSC-A v. NGFR- VioBright FITC) → CD8$^+$ *or*
226 CD4$^+$ cells (CD8-AF700 v. CD4- Pacific Blue) → Checkpoint receptor expression was analysed
227 via quarter analysis (CD27-APC-H7/ CD28-PE/ CD45RA-ECD/ CCR7-PE-Cy7). NGFR$^+$ gates
228 were set based on fully stained, vector control transduced T cells.
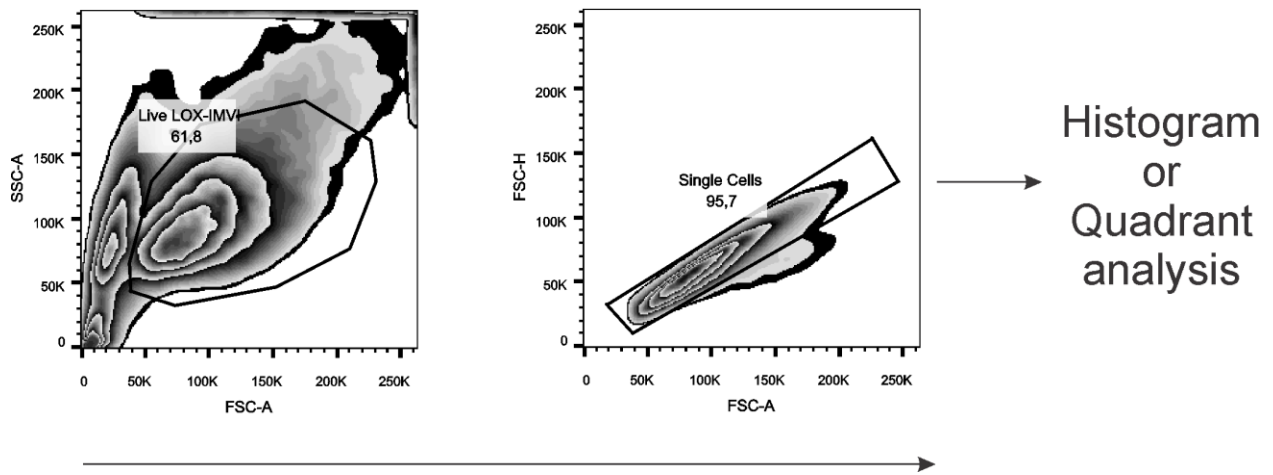
229

230

231

232

233

234

235

236   Supplementary Figure 16:

237   **Examples of gating strategies used for the analysis of flow cytometry data.** Gating strategy
238   for various adherent cell lines engineered with various surface expressing proteins. Cell gate
239   (SSC-A v. FSC-A) → singlets (FSC-H v. FSC-A) → Quadrant or Histogram analysis with
240   relevant markers

241

Test for significance in cytokine levels

	Conditions	GM-CSF	IFNg	IL-1b	IL-2	IL-4	IL-6	IL-8	IL-10	IL-12 (p70)	MCP-1	TNFa	IL-13	IL-5
Day 3	TAC-Vector	NS	NS	NS	NS	NS	NS	NS	NS	NS	N/A	NS	NS	NS
	TAC-CAR	0.00068	0.00051	NS	< 0.0001	< 0.0001	NS	NS	0.00101	NS	N/A	0.0036	0.00239	NS
	CAR-Vector	0.00013	0.00021	NS	< 0.0001	< 0.0001	NS	NS	0.0009	NS	N/A	0.00254	0.00052	NS

	Conditions	GM-CSF	IFNg	IL-1b	IL-2	IL-4	IL-6	IL-8	IL-10	IL-12 (p70)	MCP-1	TNFa	IL-13	IL-5
Day 7	TAC-Vector	NS	NS	N/A	NS	NS	NS	NS	NS	NS	NS	0.00093	NS	NS
	TAC-CAR	< 0.0001	0.00035	N/A	0.00038	0.00522	NS	0.00296	0.00061	0.00652	NS	NS	0.00025	< 0.0001
	CAR-Vector	< 0.0001	0.00035	N/A	0.00035	0.00523	NS	0.00325	0.00063	0.00867	NS	NS	0.00025	< 0.0001

Supplementary Table 1:

Statistical analysis of serum cytokine data. An unpaired t-test was used to evaluate the statistical significance of the serum cytokine data (n = 3 for each of HER2-TAC-, HER2-CAR-, and vector control T cells) presented in Figure 6. Pairwise comparisons between the three treatment groups are presented for each of the thirteen cytokines tested. P-values are shown. NS = not significant using a confidence interval of 95%. N/A denotes cases where no analysis was mathematically possible.

252

FWD-1	GGCGCGCCATGGATTTCCAGGTCCAGATTTTC
REV-1	CCCGGGGTTCAGGTCTTCTTCGCTAATC
FWD-2	ATATGGCGCGCCATGGATTTCC
REV-2	GCTGAACTTCACTCTGCAGTAAAGGGTGATAACCAG
FWD-3	ATCACCCTTTACTGCAGAGTGAAGTTCAGCAGGAG
REV-3	ATATGCTAGCTTAGCGAGGGGG
FWD-4	ATATGGATCCGTGGGGTCACCGTCTCCTCAACC
REV-4	ATATGCTAGCTTAGCGAGGGGGCAGGGC
FWD-5	CATGTGACTCCACGGAGTACCGG
REV-5	GTCCGAACGTCCACGGCAGAG
FDW-6	GGTCTTCTTCGCTAATCAGTTTCTGTTCCGGCCTGGCGGCGTGG
REV-6	CCACGCCGCCAGGCCGGAACAGAAACTGATTAGCGAAGAAGACC

253

254 Supplementary Table 2:
255 Sequence of oligos used in construction of various plasmid constructs described in materials and
256 methods.